

# Effect of Al<sub>2</sub>O<sub>3</sub> nanofiller on the electrical, thermal and structural properties of PEO:PPG based nanocomposite polymer electrolyte

A. Christina Nancy<sup>1,2</sup> · S. Austin Suthanthiraraj<sup>1</sup>

Received: 28 July 2016 / Revised: 5 December 2016 / Accepted: 4 January 2017 / Published online: 12 January 2017  
© Springer-Verlag Berlin Heidelberg 2017

**Abstract** A new series of nanocomposite polymer electrolyte (NCPE) system comprising of polyethylene oxide (PEO) and polypropylene glycol (PPG) as blended polymer host, zinc trifluoromethanesulfonate [Zn(CF<sub>3</sub>SO<sub>3</sub>)<sub>2</sub>] as dopant salt and nanocrystalline alumina [Al<sub>2</sub>O<sub>3</sub>] as filler was prepared by solution casting technique. The present system consisting of five different compositions of 87.5 wt% (PEO:PPG)–12.5 wt% Zn(CF<sub>3</sub>SO<sub>3</sub>)<sub>2</sub> + *x* wt% Al<sub>2</sub>O<sub>3</sub> [where *x* = 1, 3, 5, 7 and 9, respectively] has been thoroughly characterized by various analytical techniques such as electrical impedance spectroscopy, X-ray diffraction (XRD) studies, differential scanning calorimetry (DSC), scanning electron microscopic (SEM) analysis and linear sweep voltammetry (LSV). The maximum room temperature ionic conductivity exhibited by the NCPE was found to be  $2.1 \times 10^{-4}$  S cm<sup>-1</sup> for 3 wt% loading of Al<sub>2</sub>O<sub>3</sub> which is an order higher than that of the optimized filler-free zinc salt doped polymer electrolyte system at 298 K. The evidence of a decrease in the degree of crystallinity responsible for the enhanced conductivity was revealed by the XRD data and further confirmed by DSC and SEM results. Moreover, the electrochemical stability window of the highly conducting electrolyte matrix has been experimentally determined by linear sweep voltammetry and found to be 3.6 V which is fairly adequate for the construction of zinc primary batteries as well as zinc-based rechargeable batteries at ambient conditions.

**Keywords** Nanocomposite · PEO–PPG blend polymer · Zinc triflate · Alumina nanofiller

## Introduction

The development and employment of efficient battery materials attract tremendous technological interest in the study of material science. The earliest form of electrolytes involves the dissociation of salt molecules in a liquid solvent exhibiting an appreciably high ionic conduction. One of the advantages of these liquid electrolytes apart from their remarkably high conductivity is its ability to adapt to the volume changes within the electrode material occurring during the charging and discharging cycles. However, the limitations of liquid electrolytes such as solvent leakage, risk of fire hazard, poor mechanical strength and difficulties in waste disposal compel us to opt for an effective substitute such as solid electrolytes. Although fast ion conducting solid electrolytes display good physical and chemical stability, it is only at the expense of decreased ionic conductivity. As a result, achieving a good balance between high ionic conductivity and a broad electrochemical stability window in solid electrolytes is a great challenge in the synthesis of battery materials.

As a remarkable contribution in the field of electrolytic materials, Wright et al. in the 1970s developed polymer electrolytes synthesized by dissolving appropriate alkali salts in polyethylene oxide (PEO) matrix to serve as separators and ionic conductors in primary and rechargeable batteries [1]. These polymer electrolytes display several merits such as ease to fabricate, leak-proof nature, good mechanical strength, adaptability to volume changes during charging and discharging, high specific energy and enhanced electrochemical stability [2, 3]. It is evident from the literature that PEO–LiX complex is the most extensively studied solid polymer

✉ A. Christina Nancy  
a.christinanancy@gmail.com

<sup>1</sup> Department of Energy, University of Madras, Guindy Campus, Chennai 600025, India

<sup>2</sup> Department of Physics, Women's Christian College, Chennai 600006, India

electrolyte material [3–5]. This semi-crystalline polymer PEO with high molecular weight and high ionic conductivity envelops lithium ions present in the salt, giving rise to coordination bonds. Although these lithium batteries are crowned with several merits, the low lattice energy of lithium salts and the size of the anion retard the conductivity of the electrolyte. Moreover, factors such as toxicity, high cost and safety issues involved in the synthesis and usage of lithium batteries compel us to consider other alkali metals as viable alternatives [6–9]. A large number of polymer electrolytes involving different mobile ions, viz.  $\text{Li}^+$ ,  $\text{Na}^+$ ,  $\text{K}^+$ ,  $\text{Ag}^+$ ,  $\text{Zn}^{2+}$ ,  $\text{Mg}^{2+}$ , etc., as major charge carriers, have been investigated in the last four decades and their potential usage as electrolytes in various solid-state electrochemical power sources has also been explored [10, 11]. Recently, zinc ion conducting rechargeable batteries have received much attention and are preferred as good alternatives to lithium batteries because of its low toxicity, easy handling, abundance and non-hazardous nature. In addition, the divalent  $\text{Zn}^{2+}$  ion could replace reactive alkali metals in certain electrochemical applications too [12, 13].

On the other hand, PEO which has a helical structure with C-O and C-C bonds contains a highly ordered structure with both crystalline and amorphous phases and exhibits good complexation properties and mechanical stability. However, the crystalline phase of PEO restricts the movement of ions in the polymer electrolyte which depend on the segmental motion of the local chains [14]. Therefore, the room temperature ionic conductivity of such PEO-based electrolytes is found to be very low for practical electrochemical applications lying in the order of  $10^{-7}$  S  $\text{cm}^{-1}$ . In view of the fact that amorphous nature tends to increase the conductivity of such crystalline polymers, it is preferred to add an amorphous polymer with lower molecular weight and higher dielectric constant to the polymer host by a process called polymer blending. Blending PEO with polypropylene glycol (PPG) decreases the degree of crystallinity of the blended electrolytic system thereby increasing its ionic conductivity. However, specific disadvantage of any polymer blend system is that, on increasing the amorphous nature of the blend for enhanced conduction, the mechanical stability of the system is compromised [15].

In the recent past, a new strategy of dispersing inorganic ceramic nanofillers such as  $\text{Al}_2\text{O}_3$ ,  $\text{MgO}$ ,  $\text{Fe}_2\text{O}_3$ ,  $\text{CeO}_2$ ,  $\text{TiO}_2$ ,  $\text{SiO}_2$ ,  $\text{ZrO}_2$ , etc. in the polymer matrix is being carried out and reported [5, 16, 17]. Among the various inorganic nanofillers reported in the literature,  $\text{Al}_2\text{O}_3$  is the earliest and most extensively studied filler for PEO-based polymer electrolytes [5]. The nanofiller-doped electrolytes which are known as nanocomposite polymer electrolytes (NCPE) show superior mechanical stability, reduced degree of crystallinity, and high ionic conductivity [2, 18]. Conductivity enhancement in these electrolytes may be attributed to the  $\text{O}^{2-}/\text{OH}^-$  surface groups of the fillers which modify the network structure owing to a

reduction in the PEO reorganizing tendency and creating conducting pathways for cations along the filler surface by means of establishment of Lewis acid-base network with the mobile ions and also aid in better dissociation of the alkali salt [19]. The promising features of NCPEs over conventional liquid electrolytes attract a wide range of application in electrochemical devices and energy storage devices such as batteries, sensors, display systems and so on [6, 10].

Among the various approaches employed, polymer blending and addition of nanofillers are the two efficient ways to increase ionic conductivity and mechanical integrity of the polymer electrolytes, and hence, it was decided to employ both the techniques to uncover the most promising polymer electrolyte for several applications. Therefore, the current paper intends to report the development and characterization of a new class of NCPE consisting of PEO, PPG, zinc triflate and nano-alumina, and an extensive study of the additive effect of  $\text{Al}_2\text{O}_3$  on the electrical, thermal and structural properties of polymer electrolyte. Further, in an attempt to understand the behaviour of these nanocomposite polymer electrolytes, various analytical tools such as XRD, SEM, DSC, impedance spectroscopy and LSV have been employed for a thorough investigation.

## Experimental techniques

### Materials

Polyethylene oxide (PEO) with  $M_w = 5 \times 10^6$ , polypropylene glycol (PPG) with  $M_w = 2700$ , zinc triflate,  $\text{Zn}(\text{CF}_3\text{SO}_3)_2$  with  $M_w = 363.53$  (zinc trifluoromethanesulfonate) and nano-alumina ( $\text{Al}_2\text{O}_3$ ) with particle size less than 50 nm were procured from Sigma-Aldrich, USA, and were used as starting materials. Acetonitrile ( $\text{CH}_3\text{CN}$ ) was used as the common solvent for the preparation of thin film specimens of all the nanocomposite polymer electrolyte systems. While the specimen of PEO was dried at  $60^\circ\text{C}$  for an hour, both  $\text{Zn}(\text{CF}_3\text{SO}_3)_2$  and  $\text{Al}_2\text{O}_3$  were dried at  $100^\circ\text{C}$  for an hour prior to their use in order to eliminate any trace of moisture present, whereas PPG was used as received.

### Preparation of thin film polymer electrolytes

Thin film polymer electrolytes may be prepared by several physical and chemical methods, while the present investigation deals with the commonly employed solution casting technique. In order to obtain a series of thin film nanocomposite polymer electrolyte specimens, chosen host polymers including PEO and PPG in the ratio of 90:10 wt% were dissolved in an appropriate amount of acetonitrile by magnetically stirring until the formation of a visibly homogenous solution. Subsequently, 12.5 wt% moisture-free dopant salt namely zinc

triflate,  $\text{Zn}(\text{CF}_3\text{SO}_3)_2$ , was added to the polymer blend solution, and the solution mixture was continuously stirred at  $40^\circ\text{C}$ . In the meantime, five different concentrations involving 1, 3, 5, 7 and 9 weight percentage of dried inorganic alumina nanofillers were ultrasonically dispersed individually in the common solvent, viz. acetonitrile using a sonicator bath for 1 h at  $40^\circ\text{C}$ . Eventually, these  $\text{Al}_2\text{O}_3$  dispersed solvent solutions were incorporated in the polymer-salt matrix, and the solvent was allowed to evaporate with a constant stirring process performed at ambient conditions for 6 h. The homogeneous residual solutions thus derived were then cast onto thoroughly cleaned glass petri dishes, and the solvent was left to evaporate slowly at room temperature for 15 h. The resulting thin films were subsequently vacuum-dried at  $60^\circ\text{C}$  over a period of 24 h so as to ensure complete removal of the solvent. After subsequent vacuum drying, this procedure yielded visually homogenous free-standing nanocomposite polymer electrolyte thin films of average thickness  $160\ \mu\text{m}$ . Finally, the samples consisting of five different compositions of 87.5 wt% (PEO:PPG)–12.5 wt%  $\text{Zn}(\text{CF}_3\text{SO}_3)_2 + x$  wt%  $\text{Al}_2\text{O}_3$  ( $x = 1, 3, 5, 7$  and  $9$ ) thus prepared were designated as A1, A2, A3, A4 and A5 corresponding to 1, 3, 5, 7 and 9 wt% nano- $\text{Al}_2\text{O}_3$ , respectively, and suitably stored in vacuum desiccators for further analysis during the course of the present investigation.

### Instrumentation

The surface morphology and cross-section view of the best conducting composition of the present nanocomposite polymer electrolyte system (PEO:PPG)– $\text{Zn}(\text{CF}_3\text{SO}_3)_2$ – $\text{Al}_2\text{O}_3$  were studied using a Hitachi SU6600 model scanning electron microscope (SEM) with electron beam energy of 15 kV at room temperature for different magnifications. In this technique, the topographical image of any surface is obtained by analysing the secondary electrons scattered by the high energy electrons focused on its surface. Prior to the examination, to avoid the accumulation of static electric charges on the surface of nonconductive samples, an ultrathin layer of gold was coated on the samples by vacuum sputtering for 15 s.

The semi-crystalline nature of the series of PEO-based nanocomposite polymer electrolytes was examined using X-ray diffraction (XRD) technique to identify their structural characteristics and to investigate the relation between the observed ionic conductivity and their crystalline nature. The diffraction patterns of all five compositions of the freshly-prepared (PEO:PPG)– $\text{Zn}(\text{CF}_3\text{SO}_3)_2$ – $\text{Al}_2\text{O}_3$  thin films were recorded using a Bruker D8 Advance X-ray diffraction system with  $\text{Cu-K}_\alpha$  radiation (wavelength,  $\lambda = 1.5406\ \text{\AA}$ ) at room temperature in the scanning angle ( $2\theta$ ) range between  $10$  and  $80^\circ$  at a scan rate of  $4^\circ/\text{min}$ .

Thermal behaviour of all the specimens of NCPEs prepared was analysed using differential scanning calorimetry (DSC) performed with the aid of a NETZSCH model DSC 200F3

system. The measurements were carried out in the temperature range  $-50$  to  $150^\circ\text{C}$  in the second heating cycle at a heating rate of  $10^\circ\text{C}/\text{min}$  under nitrogen atmosphere to maintain an inert and moisture-free environment within the thermal analyser. Each of the mechanically stable thin film samples weighing 5 to 10 mg was sealed separately in closed aluminium pans, and an empty aluminium pan was used as the reference pan. Both the pans were heated simultaneously with the aid of a computer-controlled heater within the analyser.

AC impedance measurements were performed on the various compositions of (PEO:PPG)– $\text{Zn}(\text{CF}_3\text{SO}_3)_2$ – $\text{Al}_2\text{O}_3$  NCPEs system over the frequency range 20 Hz–1 MHz with an applied excitation voltage of 50 mV in the temperature range 298–333 K by means of a computer-controlled Hewlett-Packard model HP4284A Precision LCR Meter. All the polymer thin film samples under evaluation were preheated at  $60^\circ\text{C}$  for an hour prior to the complex impedance analysis to carefully remove any possible trace of undesired moisture content trapped within the polymer electrolyte specimens as well. The sample of  $160\ \mu\text{m}$  thick was suitably sandwiched between a pair of polished spring-loaded stainless steel (SS) electrodes acting as blocking electrodes thereby providing an effective contact area of  $0.5\ \text{cm}^2$  for the cell configuration. Both real and imaginary parts of impedance values of all the specimens were evaluated from the set of impedance plots obtained with the aid of in-built software loaded into the computer-controlled LCR meter with precision.

The electrochemical stability window of the best conducting sample was determined by linear sweep voltammetry (LSV) using CHI 1100A model electrochemical analyser. The three-electrode Zn/NCPE/SS cell of area  $1\ \text{cm}^2$  was constructed employing inert stainless steel disc as working electrode and zinc metal disc as both reference and counter electrodes at a scan rate of  $10\ \text{mV}/\text{s}$  from 0 to 6 V.

## Results and discussion

### Structural and morphological studies

XRD analysis is one of the common and effective analyses to investigate the apparent changes in the crystalline nature of a material. The set of room temperature XRD patterns as shown in Fig. 1a tend to reveal the structural characteristics of PEO:PPG blend polymer under consideration after it has been impregnated with 12.5 wt% zinc triflate ( $\text{Zn}(\text{CF}_3\text{SO}_3)_2$ ) and five different concentrations of nano-alumina ( $\text{Al}_2\text{O}_3$ ) involving 1, 3, 5, 7 and 9 wt%, respectively. In addition, the enlarged regions of room temperature XRD diffraction patterns obtained in the case of pure PEO, PEO:PPG blend, (PEO:PPG)– $\text{Zn}(\text{CF}_3\text{SO}_3)_2$  blended polymer electrolyte and sample A2 having 3 wt%  $\text{Al}_2\text{O}_3$  pertaining to the (PEO:PPG)–

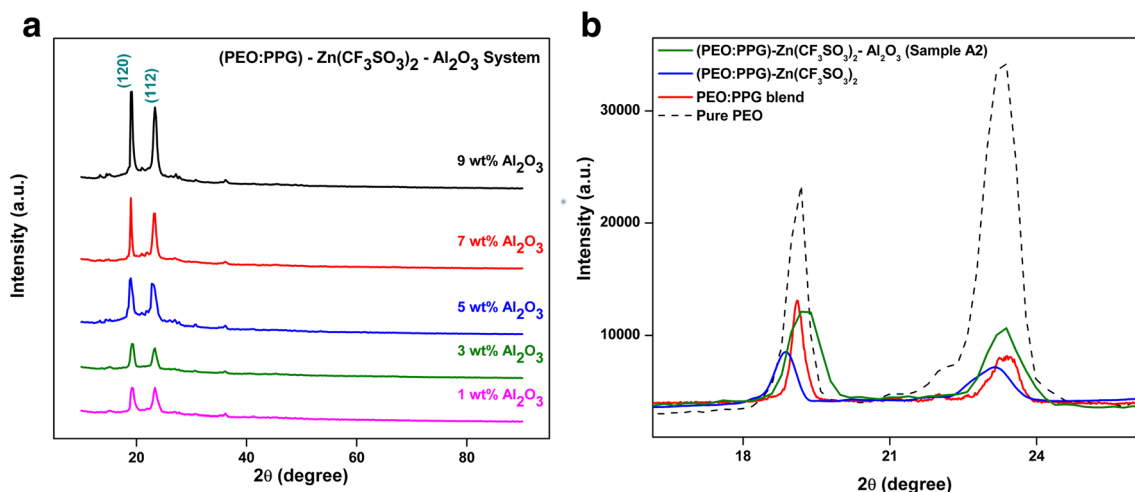


**Fig. 1** **a** Room temperature XRD patterns recorded for five different compositions of (PEO:PPG)–Zn(CF<sub>3</sub>SO<sub>3</sub>)<sub>2</sub>–Al<sub>2</sub>O<sub>3</sub> system having 1, 3, 5, 7 and 9 wt% Al<sub>2</sub>O<sub>3</sub>. **b** Room temperature XRD patterns of pure

PEO, PEO:PPG blend, (PEO:PPG)–Zn(CF<sub>3</sub>SO<sub>3</sub>)<sub>2</sub> blended polymer electrolyte and sample A2 of (PEO:PPG)–Zn(CF<sub>3</sub>SO<sub>3</sub>)<sub>2</sub>–Al<sub>2</sub>O<sub>3</sub> NCPE system

Zn(CF<sub>3</sub>SO<sub>3</sub>)<sub>2</sub>–Al<sub>2</sub>O<sub>3</sub> NCPE system are shown in Fig. 1b for the sake of better clarity of XRD results and comparison of various structural features noticed in terms of peak intensities. Two dominant peaks at 19.2 and 23.4° related to the crystalline phase of PEO [20, 21] corresponding to (120) and (112) reflection planes of a monoclinic crystal system were observed in all the five different samples of the chosen NCPE system as evident from both Fig. 1a as well as Fig. 1b. However, the relevant intensities of both these peaks varied for each composition thereby suggesting a corresponding increase or decrease in the crystalline nature of those polymer blended electrolytes under study. Figure 1b reveals the fact that the intensity of two characteristic XRD peaks observed for pure PEO sample is generally much greater than those pertaining to all the remaining polymeric systems under consideration and that the addition of PPG tends to drastically reduce the original peak intensities of pure PEO material. The addition of zinc triflate salt is found to result in a further reduction in the intensities of both these peaks, whereas the incorporation of Al<sub>2</sub>O<sub>3</sub> nanofiller beyond 3 wt% loading considerably increases peak intensities in the case of diffraction peaks around 19 and 23°. In other words, the ordered PEO structure is effectively disturbed by the addition of zinc triflate salt due to the feasibility of coordination interactions occurring between zinc ions and ether oxygen atoms. In addition, XRD patterns obtained in the case of all the chosen specimens exhibit a typical halo around 21° thus denoting the amorphous phase prevalent due to the addition of amorphous PPG into the PEO matrix. As a consequence, a significant reduction in the intensity of XRD peaks may be attributed to the feasibility of destruction of the ordered arrangement of the polymer side chains by PPG system, and hence an apparent enhancement in the amorphous phase of PEO as well [22]. It is evident from the present XRD

patterns shown in Fig. 1a that there are no peaks corresponding to the crystalline zinc triflate salt and alumina nanofiller indicating the complete dissolution and complexation of salt and filler within the five different specimens of (PEO:PPG)–Zn(CF<sub>3</sub>SO<sub>3</sub>)<sub>2</sub>–Al<sub>2</sub>O<sub>3</sub> nanocomposite polymer electrolyte system.

In addition to the above valuable information on peak position and intensity, XRD analysis also provides necessary and sufficient information pertaining to both the crystallite size and degree of crystallinity of various specimens. The values of average crystallite size (*D*) in the case of all the thin film samples have been estimated by means of XRD line broadening and Scherrer formula [23] as given by

$$D = \frac{k\lambda}{\beta \cos\theta} \quad (1)$$

where *k* is the Scherrer shape factor (*k* = 0.94),  $\lambda$  is the wavelength of X-rays used,  $\theta$  is the Bragg angle and  $\beta$  is the full width at half maxima in radians calculated using Gaussian fitting. The results revealed an average crystallite size of about 8 nm. The values of degree of crystallinity ( $\chi_c$ ) were obtained with the aid of peak separation software Origin Pro8 for all the five samples by deconvoluting the XRD peaks due to amorphous and crystalline phases [24] according to the equation:

$$\chi_c = \frac{I_c}{I_c + I_a} \quad (2)$$

where *I<sub>c</sub>* represents the total crystalline area of the observed peaks and *I<sub>a</sub>* represents the amorphous area of the observed halo in each diffraction pattern. The degree of crystallinity data thus calculated range from 41.1 to 46.8% and are tabulated in Table 1 for various compositions of the NCPE system under consideration. With the addition of ceramic alumina

**Table 1** Glass transition temperature, melting temperature, melting enthalpy and degree of crystallinity data for various samples of (PEO:PPG)–Zn(CF<sub>3</sub>SO<sub>3</sub>)<sub>2</sub>–Al<sub>2</sub>O<sub>3</sub> nanocomposite polymer electrolyte system

Sample code	Melting temperature $T_m$ (°C)	Melting enthalpy $\Delta H_m$ (J/g)	Glass transition temperature $T_g$ (°C)	Degree of crystallinity $\chi_c$ (%)	
				From XRD	From DSC
A1	69.6	88.1	–41	42.1	41.2
A2	68.6	86	–46.6	41.1	40.2
A3	70.4	90.6	–40	45.3	42.4
A4	70.9	92.8	–35.4	46	43.4
A5	71.3	93.9	–33.5	46.8	43.9

nanofiller, it is apparent from the above XRD patterns (Fig. 1a) that the structure of the polymer matrix is altered due to the reorganization of the polymer chain giving rise to a low degree of crystallinity only until 3 wt% of Al<sub>2</sub>O<sub>3</sub> nanofiller. It is remarkable to note that the crystallinity of the typical NCPE designated as A2, containing 3 wt% of Al<sub>2</sub>O<sub>3</sub> accounts to the minimum value of 41.1% which may be attributed to the Lewis acid-base interactions occurring at the EO groups of the polymer and Lewis acid sites of the nanofiller [21]. However, further increase in the Al<sub>2</sub>O<sub>3</sub> content (>3 wt%) records an increase in the degree of crystallinity due to the possible reorientation of PEO polymer chains which may tend to restrict the dipole-dipole interaction or hydrogen bonding of the polar groups near the surface in conjunction with the effect of nano-Al<sub>2</sub>O<sub>3</sub> acting as a nucleating agent thereby reducing the free volume of the polymer matrix [24, 25]. In spite of the amorphous phase introduced by the incorporation of the nanofiller, the XRD data tend to indicate that the crystalline phase of PEO is still present within the polymer electrolyte.

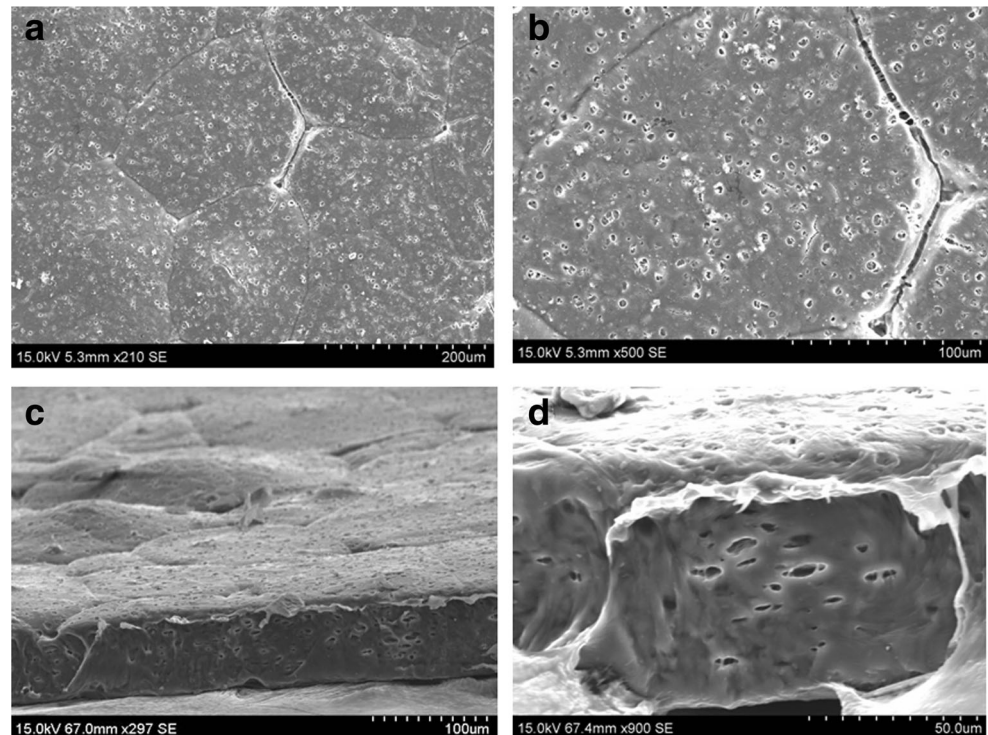
SEM is a versatile analytical tool often used to study the structural compatibility between various constituents of the NCPEs and to support the information extracted from the XRD analysis. The compatibility between the host polymer matrix, dopant salt and inorganic fillers has significant influence on the physico-chemical properties of PEO-based composite electrolytes [26]. Figure 2a–d depicts the set of SEM images observed for thin film specimen of the best conducting (PEO:PPG)–Zn(CF<sub>3</sub>SO<sub>3</sub>)<sub>2</sub>–Al<sub>2</sub>O<sub>3</sub> system designated as A2 at different magnifications facilitating the morphological investigations on its surface (Fig. 2a, b) and cross-section (Fig. 2c, d). In general, pure PEO has a rough surface with several crystalline domains of more or less equal size of spherulites [19] which signify the crystalline phase of the host polymer. In the NCPE under study, similar characteristic crystalline domains of PEO are seen, whereas it is evident from Fig. 2 that the spherulite structure is replaced by a relatively smooth surface with irregular sized small pores. This smoothing of the surface may be associated with the addition of zinc triflate and alumina nanofiller which confirms the homogeneity of the polymer electrolyte and subsequent enhancement in

observed ionic conductivity owing to the reduction in PEO crystallinity [27]. The small pores present on the homogenous surface of the specimen may have been formed due to the evaporation of the acetonitrile solvent during the preparation process. Moreover, a closer look at the observed SEM images (Fig. 2b) reveals the existence of small gaps at the boundary between the crystalline domains indicating of the existence of an amorphous phase [21]. The observed cross-sectional view of the specimen (Fig. 2c, d) reveals the presence of relatively smooth surface and non-uniform pores not just on the surface but throughout the cross section of the polymer electrolyte. All the SEM images of nanocomposite polymer electrolyte film confirm the absence of phase separation indicating an improved interaction and compatibility between the polymer blend, salt and nanofiller. Therefore, it is evident that the above micro-structural observation is in excellent agreement with XRD and DSC results which indicate an enhancement in the amorphous phase of the NCPEs with the addition of Al<sub>2</sub>O<sub>3</sub> nanofiller.

### Thermal studies

DSC measurements have been carried out on the polymer thin films to obtain qualitative information regarding the temperatures of possible phase transitions due to rearrangement of polymer chains during the application of heat. The typical DSC plots of the NCPE system under consideration are shown in Fig. 3a for all the samples with various weight percentages of alumina nanofiller. The values of glass transition temperature, melting temperature, melting enthalpy and degree of crystallinity data for (PEO:PPG)–Zn(CF<sub>3</sub>SO<sub>3</sub>)<sub>2</sub>–Al<sub>2</sub>O<sub>3</sub> system are summarized in Table 1. The observed prominent endothermic peak around 70°C in all the five specimens of NCPE system indicates the melting temperature,  $T_m$  of PEO in polymer complexes [28] and proves the existence of both crystalline and amorphous phases in the system. Interestingly, this melting peak broadens and records a drop in its intensity owing to a decrease in the area under the peak until the addition of 3 wt% of the nanofiller after which the increase in the filler content tends to increase

**Fig. 2** SEM images of (a, b) Surface morphology and (c, d) cross-sectional morphology of best conducting sample A2 at various magnifications



the melting enthalpy of the sample. This melting enthalpy plays a significant role in the determination of the crystalline nature of the polymer samples as

$$\chi_c = \frac{\Delta H_m}{\Delta H_{mp}^o} \times 100\% \quad (3)$$

where  $\chi_c$  is the degree of crystallinity,  $\Delta H_m$  represents the melting enthalpy of the sample and  $\Delta H_{mp}^o$  represents the melting enthalpy of 100% crystalline PEO = 213.1 J/g

[29]. In this PEO:PPG blended polymer system, PEO has been considered as a homopolymer for the calculation of the degree of crystallinity since PPG is essentially an amorphous polymer. The calculated values of the degree of crystallinity and melting temperature listed in Table 1 show a decline in their values until 3 wt%  $\text{Al}_2\text{O}_3$  as 40.2% and 68.6 °C, respectively, and further increase of  $\text{Al}_2\text{O}_3$  content increases their values as shown in the tabulation. This is a clear indication that the incorporation of nano- $\text{Al}_2\text{O}_3$  helps to increase the amorphous phase

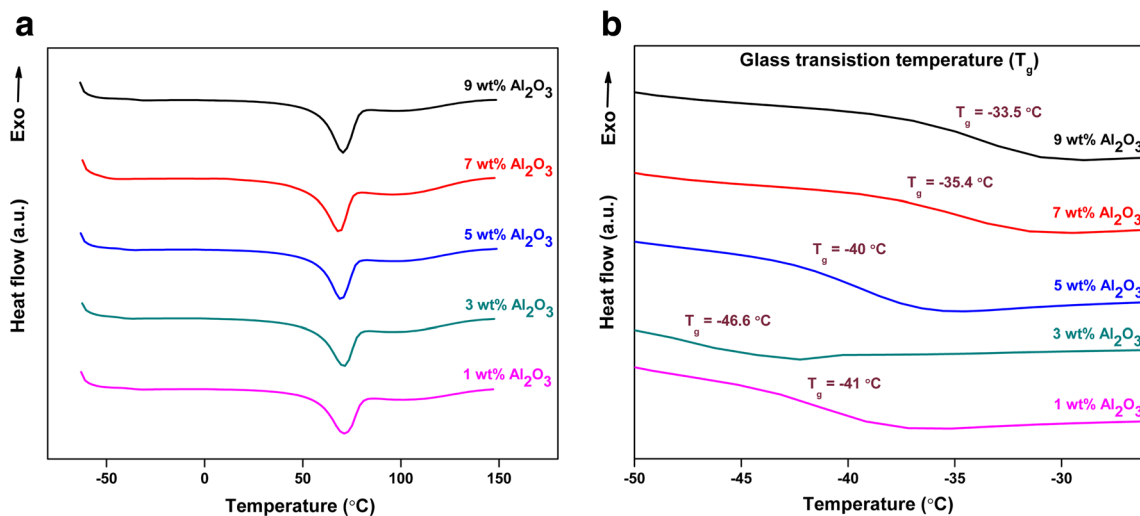


**Fig. 3** a DSC thermograms observed for various thin film samples of (PEO:PPG)- $\text{Zn}(\text{CF}_3\text{SO}_3)_2$ - $\text{Al}_2\text{O}_3$  nanocomposite polymer electrolyte system. b Glass transition temperature region magnified from the DSC

thermograms for (PEO:PPG)- $\text{Zn}(\text{CF}_3\text{SO}_3)_2$ - $\text{Al}_2\text{O}_3$  nanocomposite polymer electrolyte system

content and hence the flexibility of the polymer chains of the (PEO:PPG)–Zn(CF<sub>3</sub>SO<sub>3</sub>)<sub>2</sub> polymer electrolyte only until 3 wt% of loading of the nanofiller. The observed minimum crystallinity for the sample designated A2 appears to suggest that both zinc triflate salt and nano-Al<sub>2</sub>O<sub>3</sub> may hinder the reorganization of PEO chains through Lewis acid–base interactions by coordinating with ether oxygen atoms of PEO, Zn<sup>2+</sup> and Al<sub>2</sub>O<sub>3</sub> [26]. As evident from Table 1, the slight variation observed in the crystallinity results from DSC and XRD measurements may be due to recrystallization occurring in the DSC heating process even though the trends of the calculated data are in good agreement.

Another prominent feature noticed during the careful analysis of presently observed DSC thermograms is the occurrence of glass transition temperature ( $T_g$ ) of various specimens under consideration which is magnified and shown in Fig. 3b for the sake of clarity. Generally, in a polymer electrolyte,  $T_g$  concerns with the mobility of the polymer chain and a low  $T_g$  value is often associated with fast ion conducting behaviour [30]. A rigid chain possesses a high  $T_g$  value and the decrease in  $T_g$  helps in the effortless movement of the polymer chains; in other words,  $T_g$  measures the ability of a chain to move freely about the chain bonds, which in turn results in an increase in the conductivity. It is evident from Fig. 3b and Table 1 that glass transition temperature ( $T_g$ ) varies from –46.6 to –33.5 °C for various levels of Al<sub>2</sub>O<sub>3</sub> doping. In the case of the present system, the occurrence of the lowest value of –46.6 °C as  $T_g$  for the typical sample designated as A2 having 3 wt% Al<sub>2</sub>O<sub>3</sub> appears to suggest its more amorphous nature when compared to the remaining specimens. Excellent ionic conductivity is recorded in highly amorphous polymers when the polymer chain acquires more rapid internal modes in which bond rotations enable segmental motion to favour inter- and intra-chain ion hopping [31]. Therefore, since the segmental motion is the key determining factor for the mobility of the charge carriers, the NCPE designated as A2 is expected to exhibit an enhanced conductivity too. At higher Al<sub>2</sub>O<sub>3</sub> concentrations, that is, above 3 wt% Al<sub>2</sub>O<sub>3</sub>, a negative effect is observed and an increase in  $T_g$  is recorded. This type of behaviour involving an unfavourable increase in the value of  $T_g$  from –46.6 to –33.5 °C noticed as a result of incorporation of more than 3 wt% Al<sub>2</sub>O<sub>3</sub> nanofiller into the chosen PEO:PPG polymer blend may be attributed to the most probable blocking of ion-conducting pathways due to the feasibility of formation of higher contents of ionic aggregates and ionic clusters beyond 3 wt% of loading. These observations made from the present DSC thermograms clearly suggest that a major contribution to the improved conductivity evolves from the structural modifications associated with the blend polymer host caused by the addition of nanofiller.

## Ionic conductivity data

Ionic conductivity is generally an essential characterization technique to probe the transport properties of zinc ion conducting polymer electrolytes. Nyquist plots obtained for five different compositions of the nanocomposite polymer electrolyte system (PEO:PPG)–Zn(CF<sub>3</sub>SO<sub>3</sub>)<sub>2</sub>– $x$ Al<sub>2</sub>O<sub>3</sub> under test are shown in Fig. 4 where  $x = 1, 3, 5, 7$  and 9 wt% respectively at room temperature (298 K). The ionic conductivity is calculated by knowing the value of bulk resistance and the dimensions of the polymer films from the relation,

$$\sigma = \frac{t}{R_b A} \quad (4)$$

where  $t$  denotes the thickness of the sample film,  $A$  is the contact area of the film and  $R_b$  is the bulk resistance value obtained from the corresponding Nyquist plot. The room temperature ionic conductivity of the polymer-salt system 87.5 wt% (PEO:PPG)–12.5 wt% Zn(CF<sub>3</sub>SO<sub>3</sub>)<sub>2</sub> without the presence of alumina nanofiller was found to be  $2.3 \times 10^{-5}$  S cm<sup>-1</sup>. Therefore, the incorporation of the chosen ceramic nanofiller is expected to enhance the ionic conductivity of nanocomposite polymer electrolyte in two ways as suggested by Croce et al. [32]. Firstly, by increasing the amorphous phase of PEO to favour the transport of Zn<sup>2+</sup> cation and, secondly, by providing additional Zn<sup>2+</sup> conducting pathways at the fillers' surface through Lewis acid–base interactions within these nanocomposite polymer electrolytes [26]. Table 2 reports the room temperature ionic conductivity values for the five different samples namely A1, A2, A3, A4 and A5 with the conductivity enhancement of an order from  $10^{-5}$  to  $10^{-4}$  S cm<sup>-1</sup> when the nanofiller is added into the polymer-salt complex. Further, in order to understand the

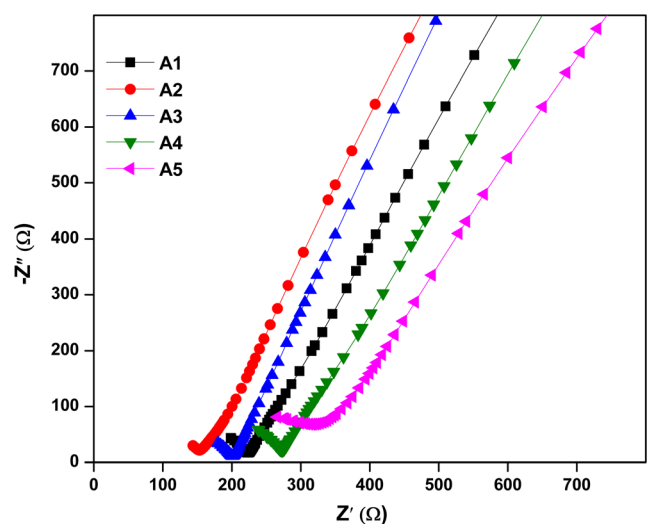


**Fig. 4** Nyquist plots for varying compositions of Al<sub>2</sub>O<sub>3</sub> in (PEO:PPG)–Zn(CF<sub>3</sub>SO<sub>3</sub>)<sub>2</sub> nanocomposite polymer electrolyte system at room temperature (298 K)

**Table 2** Bulk resistance ( $R_b$ ), room temperature ionic conductivity ( $\sigma_{298K}$ ) data and activation energy ( $E_a$ ) values for various compositions of (PEO:PPG)–Zn(CF<sub>3</sub>SO<sub>3</sub>)<sub>2</sub>–Al<sub>2</sub>O<sub>3</sub> system

Sample code	Bulk resistance $R_b$ ( $\Omega$ )	Room temperature ionic conductivity $\sigma_{298K}$ (S cm <sup>-1</sup> )	Activation energy $E_a$ (eV)
A1	224	$1.4 \times 10^{-4}$	0.48
A2	153	$2.1 \times 10^{-4}$	0.44
A3	202	$1.6 \times 10^{-4}$	0.45
A4	275	$1.2 \times 10^{-4}$	0.49
A5	317	$1 \times 10^{-4}$	0.5

effect of ceramic alumina nanofiller on the system, a plot indicating the variation of observed room temperature ionic conductivity ( $\sigma$ ) of (PEO:PPG)–Zn(CF<sub>3</sub>SO<sub>3</sub>)<sub>2</sub> electrolyte as a function of Al<sub>2</sub>O<sub>3</sub> concentration is shown in Fig. 5. The increase in ionic conductivity may be attributed to an increase in the flexibility of the NCPEs by introducing nano-Al<sub>2</sub>O<sub>3</sub> into PEO–PPG matrix, due to the high interface area between the matrix and the dispersed nano-Al<sub>2</sub>O<sub>3</sub> particles and also probably due to the increased rate of exchange of cations between ion pairs and higher aggregates and between anion associated sites and those EO sites to which the cation is weakly coordinated [33, 34]. It is interesting to note the fact that PEO and PPG contain Lewis base site of ether oxygen, while zinc triflate possesses the divalent zinc cation, which is a strong Lewis acid, and the large anion, which is a Lewis base, and the presence of Al<sub>2</sub>O<sub>3</sub> nanofiller also exhibits Lewis acid nature. Hence, there exists a huge probability that various acid-base reactions may take place within the nanocomposite polymeric system. It is clear from Fig. 4 that the intercept on the real ( $Z'$ ) axis of Nyquist plots representing the bulk resistance ( $R_b$ ) of the specimen decreases as the concentration of Al<sub>2</sub>O<sub>3</sub>

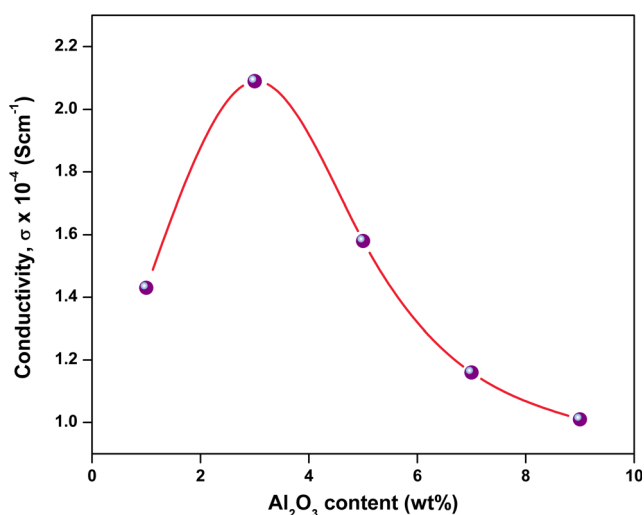


**Fig. 5** Variation of room temperature ionic conductivity of (PEO:PPG)–Zn(CF<sub>3</sub>SO<sub>3</sub>)<sub>2</sub>–Al<sub>2</sub>O<sub>3</sub> system as a function of Al<sub>2</sub>O<sub>3</sub> concentration

nanofiller is increased from 1 to 3 wt% and reaches the lowest value of  $R_b$  for the sample designated as A2 and hence record the highest ionic conductivity value. This behaviour may be associated with the introduction of alumina nanofillers whose surface would offer more physical cross-linking centres for the PEO–PPG segments and the concentration dependence of Lewis acid-base mechanism in which the presence of very low nanofiller content would favour the possibility of interactions between the acid sites of filler particles and the base centres of the polyether chain, thus increasing the cation acid sites [35]. On the other hand,  $R_b$  tends to unfavourably increase with further incorporation of Al<sub>2</sub>O<sub>3</sub> to higher values for the samples A3, A4 and A5 of this system and in turn reduce the ionic conductivity of these respective samples. This may possibly be due to an increase in ion–ion interaction that blocked the movement of Zn<sup>2+</sup> ions and reduced the conducting pathways earlier established by the Lewis acid–base interactions at the fillers' surface [36]. Excellent correlation between  $T_g$  values, degree of crystallinity values derived from both XRD and DSC measurements and the present ionic conductivity values strongly suggests that the sample containing 3 wt% Al<sub>2</sub>O<sub>3</sub>, viz., A2 is evidently the best conducting sample of the NCPE system under consideration with an increased amorphous nature and enhanced segmental mobility in its polymer chains.

In order to explore the mechanism of ionic conduction in the new class of nanocomposite polymer electrolytes, the temperature-dependent ionic conductivity data have been obtained. Fig. 6 shows the set of Arrhenius plots of all five specific polymer electrolyte samples, viz. A1, A2, A3, A4 and A5, in the temperature range 298–333 K, and the linear relation between ionic conductivity and temperature records no phase transition in the NCPEs with the addition of nano-

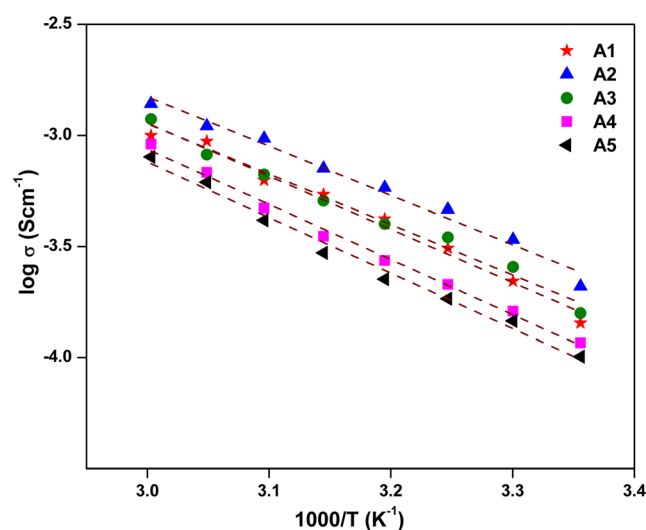


**Fig. 6** Temperature-dependent ionic conductivity plots obtained for various compositions of (PEO:PPG)–Zn(CF<sub>3</sub>SO<sub>3</sub>)<sub>2</sub>–Al<sub>2</sub>O<sub>3</sub> system over the temperature range 298–333 K



$\text{Al}_2\text{O}_3$  filler. All these ionic conductivity values have been extracted from the impedance spectroscopic measurements taken during the heating cycle. This type of linear variation noticed in  $\log \sigma$  vs.  $1000/T$  plot clearly suggests an Arrhenius-type of thermally activated process represented by

$$\sigma = \sigma_0 \exp(-E_a/kT) \quad (5)$$

where  $\sigma_0$  is the pre-exponential factor,  $E_a$  is the activation energy,  $k$  is the Boltzmann constant and  $T$  is the absolute temperature. The magnitude of ionic conductivity was found to increase linearly with an increase in temperature for all compositions of the nanocomposite polymer electrolyte system. This temperature-dependence feature and enhancement in ionic mobility may be explained on the basis of ion transport mechanism occurring through the various coordinating sites, local structural relaxation and segmental motion of the polymer chain [37]. Thus, the observed Arrhenius behaviour of the polymer system could be satisfactorily explained on the basis of free volume theory. As the temperature increases, the polymer segments would acquire sufficient vibrational energy to push the neighbouring atoms apart to create a small free space around its own volume owing to the enhanced vibrational motion of the polymer segments [37, 38]. Therefore, such free volume created around the polymer segments may aid in the increase of ion mobility i.e.  $\text{Zn}^{2+}$  ion mobility and ionic conductivity increases due to hopping mechanism via segmental motion of polymer chain.

The activation energy values ( $E_a$ ) of different compositions of  $\text{Al}_2\text{O}_3$ -doped polymer electrolytes named A1, A2, A3, A4 and A5 were calculated from the slopes of linear fit of Arrhenius plots of NCPE system from Fig. 6 and are listed in Table 2. In general, activation energy is the energy required by the mobile  $\text{Zn}^{2+}$  ions to hop from one site to another, breaking the coordination between the polymer matrix and the nanofiller [9]. From Table 2, it is seen that the activation energy is found to decrease gradually until 3 wt%  $\text{Al}_2\text{O}_3$  filler concentration, confirming the increase in amorphous nature of polymer electrolyte. However, for higher concentrations of the nanofiller, the activation energy shows a corresponding gradual increase with respect to the filler concentration. It is quite evident that ionic conductivity is inversely related to the activation energy and hence the sample having the lowest  $E_a$  is expected to correspond to the highest conducting composition. Interestingly, the sample A2 exhibiting the highest ionic conductivity shows the lowest activation energy value of 0.44 eV too.

### Electrochemical stability window

A wide electrochemical stability window of nanocomposite polymer electrolytes is a key factor in the fabrication of electrochemical devices that may be calculated by means of linear

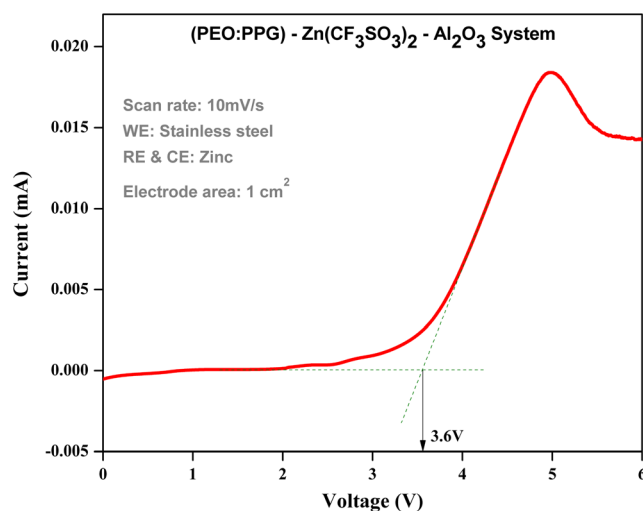


**Fig. 7** Linear sweep voltammogram of the best conducting sample A2 at 298 K

sweep voltammetry (LSV). The irreversible onset of the current determines the electrolyte breakdown voltage, which reveals the electrochemical stability of the system where no oxidation or reduction takes place. Figure 7 shows the voltammogram obtained for the best conducting sample designated as A2 with 3 wt%  $\text{Al}_2\text{O}_3$  in (PEO:PPG)– $\text{Zn}(\text{CF}_2\text{SO}_3)_2$  system in a Zn/A2/SS cell at 25°C. Anodic current was visibly negligible almost up to 2.6 V beyond which the onset of current begins as potential increases and the anodic current gradually increases until 5 V where total decomposition of the nanocomposite electrolyte specimen occurs. This onset of anodic current may be attributed to the oxidation of triflate anion followed by the degradation of the polymer chains beyond 2.6 V as suggested by Scrosati [39]. Further, the absence of negative current also indicates that there was no decomposition on the working stainless steel electrode. Generally, the electrolyte stability is considered to be the point of intersection of two extrapolated lines of the high-voltage linear current trace and the low-voltage zero current trace parallel to the  $x$ -axis. From the voltage versus current plot, it is clearly evident that the electrochemical stability window of the present system is only up to 3.6 V which is fairly adequate and comparable with earlier reports so as to construct zinc-based primary as well as secondary batteries [9, 40–43].

### Conclusion

In essence, the results of this study have revealed the effect of ceramic nano-alumina concentration on the morphology, structural, thermal, electrical and electrochemical properties of the newly developed (PEO:PPG)– $\text{Zn}(\text{CF}_2\text{SO}_3)_2$ – $\text{Al}_2\text{O}_3$  NCPE system prepared by simple solution casting technique. As evident from SEM, XRD and DSC measurements, the decrease in crystallinity,  $T_g$ ,  $T_m$ , and  $E_a$  until the addition of

3 wt% Al<sub>2</sub>O<sub>3</sub> confirms the increased amorphous phase content and segmental flexibility owing to the conductivity enhancement, and on further addition of the nanofiller, there is a gradual reduction in the conductivity values as reported. The ionic conductivity and activation energy for the best conducting composition of the polymer electrolyte corresponding to 3 wt% doping of Al<sub>2</sub>O<sub>3</sub> are determined to be  $2.1 \times 10^{-4}$  S cm<sup>-1</sup> and 0.44 eV, respectively, at 298 K. These results offer further evidence that ionic conductivity of the polymer electrolyte system is controlled by segmental motions of the polymer chain and ion hopping mechanism at Lewis acid-base sites and at elevated temperatures exhibit Arrhenius behaviour which was satisfactorily explained on the basis of free volume theory. Complex impedance studies and linear sweep voltammetry indicate the existence of electrochemical equilibrium between zinc metal and Zn<sup>2+</sup> ions in the NCPE. Moreover, these nano-aluminadoped PEO:PPG blend electrolytes exhibit satisfactory electrochemical stability (3.6 V), suggesting that they are promising materials for zinc batteries.

**Acknowledgements** We acknowledge the characterization facility provided for SEM analysis by the National Centre for Nanoscience and Nanotechnology, University of Madras.

## References

- Fenton DE, Parker JM, Wright PV (1973) Complexes of alkali metal ions with poly(ethylene oxide). *Polymer* 14:589. doi:10.1016/0032-3861(73)90146-8
- Liang B, Tang S, Jiang Q, Chen C, Chen X, Li S, Yan X (2015) Preparation and characterization of PEO-PMMA polymer composite electrolytes doped with nano-Al<sub>2</sub>O<sub>3</sub>. *Electrochim Acta* 169:334–341. doi:10.1016/j.electacta.2015.04.039
- Klongkan S, Pumchusak J (2015) Effects of nano alumina and plasticizers on morphology, ionic conductivity, thermal and mechanical properties of PEO-LiCF<sub>3</sub>SO<sub>3</sub> solid polymer electrolyte. *Electrochim Acta* 161:171–176. doi:10.1016/j.electacta.2015.02.074
- Sim LH, Gan SN, Chan CH, Yahya R (2010) ATR-FTIR studies on ion interaction of lithium perchlorate in polyacrylate/poly(ethylene oxide) blends. *Spectrochim Acta A Mol Biomol Spectrosc* 76:287–292. doi:10.1016/j.saa.2009.09.031
- Jung S, Kim DW, Lee SD, Cheong M, Nguyen DQ, Cho BW, Kim SH (2009) Fillers for solid-state polymer electrolytes: highlight. *Bull Kor Chem Soc* 30:2355. doi:10.5012/bkcs.2009.30.10.2355
- Sownthari K, Suthanthiraraj SA (2013) Synthesis and characterization of an electrolyte system based on a biodegradable polymer. *Express Polym Lett* 7:495–504. doi:10.3144/expresspolymlett.2013.46
- Kumar GG, Munichandraiah N (2000) Effect of plasticizers on magnesium-poly(ethylene oxide) polymer electrolyte. *J Electroanal Chem* 495:42–50
- Kumar GG, Sampath S (2004) Spectroscopic characterization of a gel polymer electrolyte of zinc triflate and polyacrylonitrile. *Polymer* 45:2889–2895. doi:10.1016/j.polymer.2004.02.053
- Sownthari K, Suthanthiraraj SA (2014) Preparation and properties of a gel polymer electrolyte system based on poly-ε-caprolactone containing 1-ethyl-3-methylimidazolium bis (trifluoromethylsulfonyl)imide. *J Phys Chem Solids* 75:746–751. doi:10.1016/j.jpcs.2014.02.003
- Caramia V, Bayer SI, Anyfantis GC, Ruffilli R, Ayadi F, Martiradonna L, Cingolani R, Athanassiou A (2013) Tailoring the morphology of poly(ethylene oxide)/silver triflate blends: from crystalline to self-assembled nanofibrillar structures. *Nanotechnology* 24:055602. doi:10.1088/0957-4484/24/5/055602
- Agrawal RC, Pandey GP (2008) Solid polymer electrolytes: material designing and all-solid-state battery applications: an overview. *J Phys D Appl Phys* 41:223001. doi:10.1088/0022-3727/41/22/223001
- Narayanan NSV, Ashokraj BV, Sampath S (2010) Ambient temperature, zinc ion-conducting, binary molten electrolyte based on acetamide and zinc perchlorate: application in rechargeable zinc batteries. *J Colloid Interface Sci* 342:505–512. doi:10.1016/j.jcis.2009.10.034
- Johnsi M, Suthanthiraraj SA (2016) Electrochemical and structural properties of a polymer electrolyte system based on the effect of CeO<sub>2</sub> nanofiller with PVDF-co-HFP for energy storage devices. *Ionics*. doi:10.1007/s11581-016-1637-x
- Sengwa RJ, Dhatarwal P, Choudhary S (2014) Role of preparation methods on the structural and dielectric properties of plasticized polymer blend electrolytes: correlation between ionic conductivity and dielectric parameters. *Electrochim Acta* 142:359–370. doi:10.1016/j.electacta.2014.07.120
- Paulmer RDA, Kulkarni AR (1994) Synthesis and conductivity behavior of ternary PEO-PPG-NaClO<sub>4</sub> amorphous blends. *Solid State Ionics* 68:243–247. doi:10.1016/0167-2738(94)90182-1
- Stephan AM, Nahm KS (2006) Review on composite polymer electrolytes for lithium batteries. *Polymer* 47:5952–5964. doi:10.1016/j.polymer.2006.05.069
- Pitawala HMJC, Dissanayake MAKL, Seneviratne VA (2007) Combined effect of Al<sub>2</sub>O<sub>3</sub> nano-fillers and EC plasticizer on ionic conductivity enhancement in the solid polymer electrolyte (PEO)<sub>9</sub>LiTf. *Solid State Ionics* 178:885–888. doi:10.1016/j.ssi.2007.04.008
- Johan MR, Shy OH, Ibrahim S, Yassin SMM, Hui TY (2011) Effects of Al<sub>2</sub>O<sub>3</sub> nanofiller and EC plasticizer on the ionic conductivity enhancement of solid PEO-LiCF<sub>3</sub>SO<sub>3</sub> solid polymer electrolyte. *Solid State Ionics* 196:41–47. doi:10.1016/j.ssi.2011.06.001
- Suthanthiraraj SA, Vadivel MK (2012) Electrical and structural properties of poly (ethylene oxide)/silver triflate polymer electrolyte system dispersed with MgO nanofillers. *Ionics* 18:385–394. doi:10.1007/s11581-011-0637-0
- Xi J, Tang X (2004) Nanocomposite polymer electrolyte based on poly(ethylene oxide) and solid super acid for lithium polymer battery. *Chem Phys Lett* 393:271–276. doi:10.1016/j.cplett.2004.06.054
- Amudha S, Suthanthiraraj SA (2015) Silver ion conducting characteristics of a polyethylene oxide-based composite polymer electrolyte and application in solid state batteries. *Adv Mater Lett* 6(10): 874–882. doi:10.5185/amlett.2015.5831
- Ahmed EA, Abdallah BW, Mohamed ME, Ahmed MM (2012) Preparation, characterizations and conductivity of composite polymer electrolytes based on PEO-LiClO<sub>4</sub> and Nano ZnO filler. *Bull Kor Chem Soc* 33(9):2949–2954. doi:10.5012/bkcs.2012.33.9.2949
- Guinier A (1994) X-ray diffraction in crystals, imperfect crystals and amorphous bodies. Dover Publications, New York
- Hyun J (2001) A new approach to characterize crystallinity by observing the mobility of plasma treated polymer surfaces. *Polymer* 42:6473–6477. doi:10.1016/S0032-3861(01)00116-1
- Jogea P, Kanchan DK, Sharma P, Gondaliya N (2013) Effect of nano-filler on electrical properties of PVA-PEO blend polymer electrolyte. *Indian J Pure Ap Phy* 51(5):350–353
- Xi J, Qiu XQ, Cui M, Tang X, Zhu W, Chen L (2006) Enhanced electrochemical properties of PEO-based composite polymer

- electrolyte with shape-selective molecular sieves. *J Power Sources* 156:581–588. doi:10.1016/j.jpowsour.2005.06.007
27. Chu PP, Reddy MJ, Kao HM (2003) Novel composite polymer electrolyte comprising mesoporous structured SiO<sub>2</sub> and PEO/Li. *Solid State Ionics* 156:141. doi:10.1016/S0167-2738(02)00582-9
  28. Akhtar MS, Kim UY, Choi DJ, Yang OB (2010) Effect of electron beam irradiation on the properties of polyethylene oxide–TiO<sub>2</sub> composite electrolyte for dye sensitized solar cells. *Mater Sci Forum* 658:161–164. doi:10.4028/www.scientific.net/MSF.658.161
  29. Dey A, Karan S, De SK (2010) Molecular interaction and ionic conductivity of polyethylene oxide–LiClO<sub>4</sub> nanocomposites. *J Phys Chem Solids* 71:329–335
  30. Ibrahim S (2012) Johan MR (2012) Thermolysis and conductivity studies of poly(ethylene oxide) (PEO) based polymer electrolytes doped with carbon nanotube. *Int J Electrochem Sci* 7:2596–2615
  31. Vignarooban K, Dissanayake MAKL, Albinsson I, Mellander BE (2015) Ionic conductivity enhancement in PEO:CuSCN solid polymer electrolyte by the incorporation of nickel-chloride. *Solid State Ionics* 278:177–180. doi:10.1016/j.ssi.2015.06.014
  32. Croce F, Appetecchi GB, Persi L, Scrosati B (1998) Nanocomposite polymer electrolytes for lithium batteries. *Nature* 394:456–458. doi:10.1038/28818
  33. Ferry A, Jacobsson P, Stevens JR (1996) Studies of ionic interactions in poly(propylene glycol)4000 complexed with triflate salts. *J Phys Chem* 100:12574–12582. doi:10.1021/jp960366r
  34. Xue Z, He D, Xie X (2015) Poly(ethylene oxide)-based electrolytes for lithium ion batteries. *J Mater Chem A* 3:19218. doi:10.1039/c5ta03471j
  35. Suthanthiraraj SA, Kumar R, Paul BJ, Mathew V (2011) Electrical conductivity and dielectric behaviour of PPG<sub>4</sub>–AgCF<sub>3</sub>SO<sub>3</sub>:Al<sub>2</sub>O<sub>3</sub> nanocomposite gel polymer electrolyte system. *J Solid State Electrochem* 15:561–570. doi:10.1007/s10008-010-1112-y
  36. Shanmukaraj D, Murugan R (2005) Characterization of PEG:LiClO<sub>4</sub> + SrBi<sub>4</sub>Ti<sub>4</sub>O<sub>15</sub> nanocomposite polymer electrolytes for lithium secondary batteries. *J Power Sources* 149:90–95. doi:10.1016/j.jpowsour.2005.02.008
  37. Kondamareddy KK, Ravi M, Pavani Y, Bhavani S, Sharma AK, Rao VVRN (2011) Investigations on the effect of complexation of NaF salt with polymer blend (PEO/PVP) electrolytes on ionic conductivity and optical energy band gaps. *Physica B* 406:1706–1712. doi:10.1016/j.physb.2011.02.010
  38. Pillai PCK, Khurana P, Tripathi A (1986) Dielectric studies of poly(methyl methacrylate)/polystyrene double layer system. *J Mater Sci Lett* 5:629–632. doi:10.1007/BF01731531
  39. Scrosati B (1987) Electrode kinetics and electrochemical cells. In: Mac Callum JR, Vincent CA (eds) *Polymer Electrolyte Reviews*. Elsevier, New York, 1: 315–345
  40. Xu JJ, Ye H, Huang J (2005) Novel zinc ion conducting polymer gel electrolytes based on ionic liquids. *Electrochem Commun* 7:1309–1317. doi:10.1016/j.elecom.2005.09.011
  41. Häupler B, Rossel C, Sohwenke AM, Winsberg J, Schmidt D, Wild A, Schubert US (2016) Aqueous zinc-organic polymer battery with a high rate performance and long lifetime. *NPG Asia Materials* 8:e283. doi:10.1038/am.2016.82
  42. Li Y, Dai H (2014) Recent advances in zinc–air batteries. *Chem Soc Rev* 43:5257–5275. doi:10.1039/c4cs00015c
  43. Huang J, Yang Z, Feng Z, Xie X, Wen X (2016) A novel ZnO@Ag@Polypyrrole hybrid composite evaluated as anode material for zinc-based secondary cell. *Nature: Scientific Reports* 6:24471. doi:10.1038/srep24471